S. Moussaddy, S. Aryal, and J. Maisonneuve, "Specific energy analysis of using fertilizer-based liquid desiccants to dehumidify indoor plant environments," Applied Thermal Engineering (in press). https://doi.org/10.1016/j.applthermaleng.2023.121849

Specific Energy Analysis of Using Fertilizer-Based Liquid Desiccants to Dehumidify Indoor Plant Environments

*Sarah Moussaddy, Sandeep Aryal, Jonathan Maisonneuve**

Department of Mechanical Engineering, Oakland University, Rochester, Michigan, 48309-4479, United States

*maisonneuve@oakland.edu, (248) 370-2657

ABSTRACT

Controlling humidity in indoor plant environments is crucial to plant growth, but traditional dehumidification methods can be energy intensive. In this study, we evaluate the energy efficiency of a novel dehumidification concept that uses cold concentrated fertilizer solution as a liquid desiccant agent. This closes the water cycle by recovering water vapor for plant fertigation, and eliminates the need for energy-intensive desiccant regeneration. A theoretical transport model is used to conduct a parametric analysis of the specific energy performance of the system in response to desiccant temperature and other operating conditions. Specific energy of dehumidification is defined here as the ratio of the cooling load to the water vapor removal. Minimum specific energy results between 0.16-0.24 Wh/g are achieved at liquid desiccant temperatures between 7-14 °C. These results compare very favorably with other dehumidification technologies on the market, and satisfy new energy efficiency standards for indoor plant cultivation. The vapor flux associated with

S. Moussaddy, S. Aryal, and J. Maisonneuve, "Specific energy analysis of using fertilizer-based liquid desiccants to dehumidify indoor plant environments," Applied Thermal Engineering (in press). https://doi.org/10.1016/j.applthermaleng.2023.121849

the minimum specific energy ranged from 1.2-1.6 g/m^2/h. Controlling liquid desiccant temperature is shown to be critical to achieving high dehumidification rates at optimal specific energies. These encouraging results suggest that future research and development along this track can contribute to energy efficient greenhouse cultivation for sustainable food production.

GRAPHICAL ABSTRACT

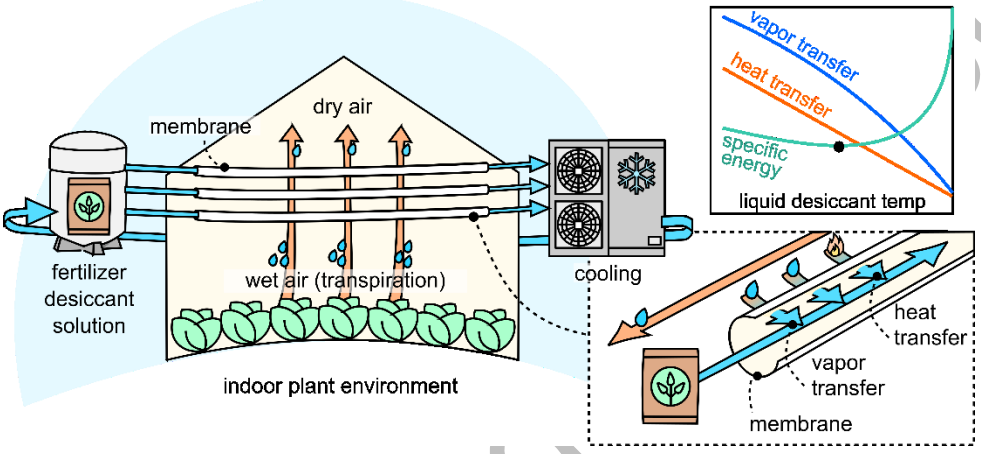

Keywords: Liquid desiccant; Dehumidification; Greenhouse; Controlled-Plant Environment; Membrane.

1. Introduction

Controlled plant environments, such as indoor farms, greenhouses, and grow chambers, have great potential to increase global food security. Such plant systems can dramatically increase crop yields and nutritional quality, reduce risks of crop failure, mitigate environmental impacts, and improve the efficiency of water, fertilizer, and energy inputs [1-3]. Much of the benefit of indoor plant environments is achieved by careful control of the plant microclimate, including indoor

humidity levels [4-5]. This is important because excessive humidity can lead to inadequate nutrient uptake, disease, and poor flowering and fruiting, while insufficient humidity can lead to high transpiration and wilting.

To maintain target humidity levels, it is necessary to remove water vapor at approximately the same rate as plant evapotranspiration [6]. While this can sometimes be achieved with fresh air ventilation, it is often preferable to operate indoor farms as closed systems, so as to reduce heating and cooling costs, and eliminate vectors for pests and other contaminants. For such closed plant environments, dehumidification is usually handled by a conventional air conditioning condenser for direct water removal [7, 8]. Alternatively, a variety of desiccant cycles have also been proposed in recent years [9-15]. With all of these technologies, one of the primary challenges is to reduce energy intensity, so as to reduce operating costs.

One measure of energy efficiency is to consider the amount of energy consumed per unit of water vapor removed from the environment, a metric known as the specific energy of dehumidification. Recent publications have reported specific energy results between 0.3-0.9 Wh/g for a variety of lab-scale vapor compression and liquid desiccant cycles operating under optimized conditions [16-18]. On the other hand, current state-of-the-art commercial packages typically require closer to 1-2 Wh/g [19]. For comparison, recent indoor farming regulations require 0.37-0.55 Wh/g [20, 21]. This suggests that improvements are needed in the efficiency of current state-of-the-art dehumidification technology.

In an effort to improve the energy efficiency of greenhouse dehumidification, we recently introduced the novel concept of using concentrated fertilizer solution as a liquid desiccant agent [22]. Figure 1 illustrates one embodiment of the concept in a membrane-based dehumidification

process. As shown, fertilizer solution is circulated through a membrane module where the low vapor pressure of the cool concentrated desiccant draws water vapor across the membrane, out of the indoor air. A chiller is used to remove the heat of condensation released from the phase change of water vapor that occurs on the desiccant surface, and thereby maintains a relatively cool fertilizer desiccant with low vapor pressure. When fertilizer solution is sufficiently diluted, it is replaced by a fresh batch of fertilizer, and then delivered directly to plants where it provides valuable nutrients in addition to closing the water cycle by recycling water vapor for irrigation. The concept was experimentally validated in our previous work, and dehumidification was confirmed across a range of typical greenhouse conditions using a variety of common fertilizers [22].

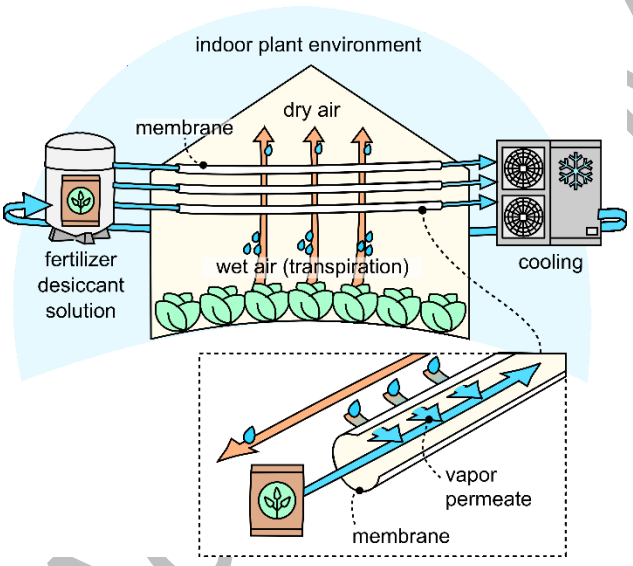

Figure 1. Water vapor permeate can be drawn from a humid air stream across a selective polymer membrane by a vapor pressure gradient established by a concentrated fertilizer-based liquid desiccant solution. This process can be used to dehumidify indoor plant environments and recycle water vapor for plant fertigation. A water-cooled chiller is used to maintain the fertilizer desiccant temperature.

S. Moussaddy, S. Aryal, and J. Maisonneuve, "Specific energy analysis of using fertilizer-based liquid desiccants to dehumidify indoor plant environments," Applied Thermal Engineering (in press). https://doi.org/10.1016/j.applthermaleng.2023.121849

A more detailed process and psychrometric diagram is also provided in Figure 2. As show, the principal advantage of the proposed dehumidification process is that it avoids the need for overcooling air to the dewpoint and then re-heating as with conventional air conditioning, and it avoids the need for thermal regeneration and then re-cooling of the liquid desiccant solution as with typical liquid desiccant processes. Therefore, while important energy savings are theoretically possible, no systematic analysis of the system's specific energy of dehumidification has yet been published in the scientific literature.

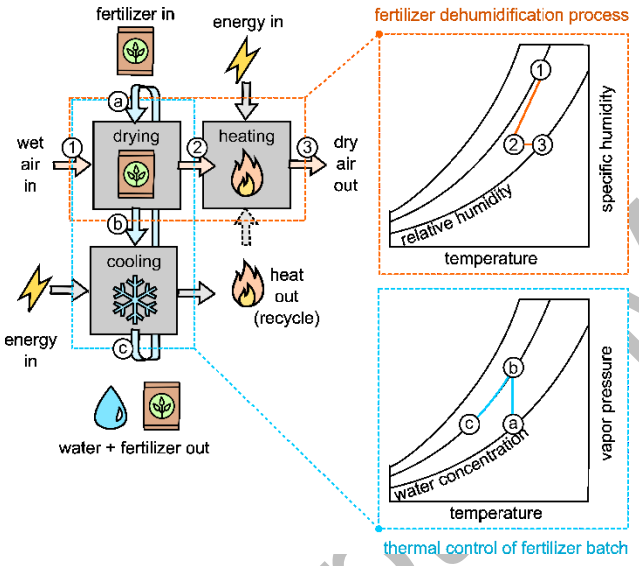

Figure 2. Process and psychrometric diagrams of fertilizer dehumidification system. (1)-(2): Humidity is absorbed by cool fertilizer liquid desiccant solution, reducing air humidity and reducing temperature due to thermal diffusion. (2)-(3): Air is reheated to ambient temperatures via a heat pump or from waste heat. (a)-(b): Fertilizer desiccant solution is diluted as water vapor is absorbed, reducing its concentration and increasing its vapor pressure. (b)-(c): Fertilizer solution at the new concentration is cooled to restore the target vapor pressure.

The purpose of this study is therefore to evaluate the theoretical specific energy of dehumidification for fertilizer-based liquid desiccant dehumidification. This builds on our previous work, which introduced the concept and provided evidence of successful

dehumidification but which importantly did not include any evaluation of the concept's energy efficiency [22]. This is the gap that this study will address. For the first time, this important performance metric will be studied here and provide insight into the potential for this technology to compete with other dehumidification systems. Fundamental mass and heat transport dynamics of the process are defined, and a numerical model is validated and then used to simulate energy performance in response to a range of operating conditions and a selection of membrane properties.

2. Theory

2.1. Specific Energy of Dehumidification

In a membrane-based dehumidification system, a polymer core separates concentrated desiccant solution from a humid air feed stream as shown in Figure 3. Water vapor from the air stream migrates to the membrane's surface, diffuses through it, and then desorbs and condenses on the liquid desiccant surface due to a differential vapor pressure between air stream and the liquid desiccant solution.

S. Moussaddy, S. Aryal, and J. Maisonneuve, "Specific energy analysis of using fertilizer-based liquid desiccants to dehumidify indoor plant environments," Applied Thermal Engineering (in press). https://doi.org/10.1016/j.applthermaleng.2023.121849

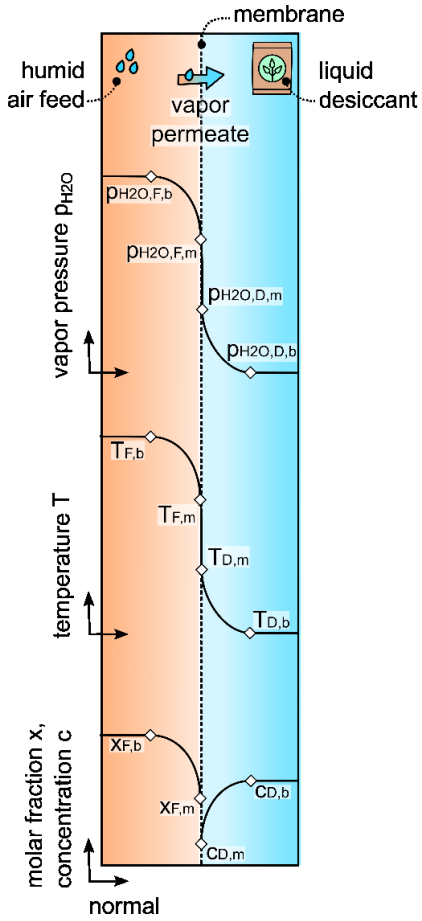

Figure 3. The water vapor pressure gradient difference between the liquid desiccant and the humid feed air drives the vapor flux in a membrane-based liquid desiccant dehumidification process. The vapor pressure difference across the membrane is determined by the non-linear temperature and concentration gradients.

Because the driving vapor pressure is strongly dependent on temperature, it is generally necessary to maintain cool liquid desiccant. This is especially important in the proposed fertilizer-based liquid desiccant process, where temperature is used to maintain the target vapor pressure, even as the batch of fertilizer solution is diluted. This thermal gradient across the membrane improves the rate of water vapor transfer, but also leads to heat transfer, and the associated thermal load must be managed by actively cooling the liquid desiccant. The result of these dynamics is a tradeoff between the rate of water vapor mass transfer and the rate of thermal energy transfer,

which are both proportional to desiccant temperature. The ratio of these two dynamics can be expressed as the specific energy of dehumidification *e*, as defined in equation er1), and optimized as a function of temperature, as illustrated in Figure 4.

$$e = \frac{\Delta Q}{\Delta m} \quad (1)$$

Where ΔQ is the amount of heat transferred to the liquid desiccant, which is the cooling load, and Δm is the amount of water removed from the humid air, both of which are defined in equations (2) and (10). Because many technologies can handle cooling loads with coefficients of performance greater than unity, it is also helpful to consider the specific energy normalized over the coefficient of performance, i.e. e / COP. Where COP is defined as the ratio of heat out relative to work in (i.e. $COP = \Delta Q$ / ΔW).

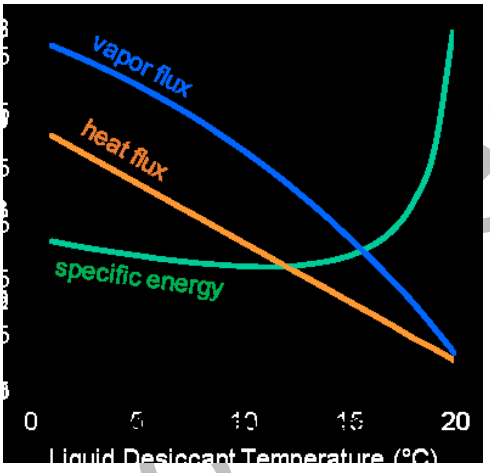

Figure 4. Water vapor flux and thermal energy flux towards the liquid desiccant solution are both increased by cool desiccant temperatures. The balance of these two-competing metrics can be expressed as the specific energy of dehumidification *e* and optimized as a function of temperature.

2.2. Vapor Transfer Across the Membrane

S. Moussaddy, S. Aryal, and J. Maisonneuve, "Specific energy analysis of using fertilizer-based liquid desiccants to dehumidify indoor plant environments," Applied Thermal Engineering (in press). https://doi.org/10.1016/j.applthermaleng.2023.121849

In a membrane-based dehumidification system, water vapor transfer from humid feed air towards concentrated liquid desiccant is driven by diffusion along a vapor pressure gradient. When normalized per unit membrane surface area, the rate of water vapor transfer can be expressed as vapor flux *J*.

$$J = \frac{\Delta \dot{m}}{a} = \dot{m}_{diffusion} \tag{2a}$$

$$J = \frac{\Delta \dot{m}}{a} = K\, \Delta p_{H2O} \tag{2b}$$

Where *a* is the membrane surface area, *K* is the mass transfer coefficient, and Δp_{H2O} is the vapor pressure difference across the membrane and fluid boundary layers. The vapor pressure of the humid feed air can be obtained as a fraction of atmospheric pressure as per Dalton's law or as a fraction of the saturation pressure, as described in equation (3). The vapor pressure of the liquid desiccant solution can be obtained from the Kohler equation [23, 24], as described in equation (4).

$$p_{H2O,F} = x\, p = rh\, p_o \tag{3}$$

$$p_{H2O,D} = p_o\, exp\left(\frac{V_m}{R\, T}(p - \pi)\right) \tag{4}$$

Where *x* is the mole fraction of water vapor, *p* is pressure, *rh* is the relative humidity, and p_o is the equilibrium vapor pressure, *R* is the gas constant, V_m is the molar volume of water, *T* is temperature, and π is osmotic pressure.

While other models have also been proposed, the equilibrium vapor pressure p_o and the osmotic pressure π, can be classically obtained from the Antoine equation and the Van't Hoff equation.

$$p_o = 10^{\left(A_o - \frac{B_o}{C_o + T}\right)} \tag{5}$$

$$\pi = i\, R\, T\, c \tag{6}$$

Where A_o, B_o, and C_o are empirical constants, i is the number of ions, and c is the ion concentration.

In cases where a rough estimate of flux is satisfactory, the vapor pressures in equations (3) and (4) can be calculated from the properties, temperatures, and concentrations of the bulk fluids. However, in cases where a more accurate model of flux is desired, boundary layer dynamics should be considered, to obtain vapor pressures as a result of temperatures, concentrations, and other fluid properties at the membrane surfaces.

In this case, a lumped element approach is taken and vapor diffusion across the membrane and also the fluid boundary layers is considered. This is done by considering the water vapor pressure difference Δp_{H2O} across each of their respective mass transfer coefficients K. Where K_m, K_F, and K_D are mass transfer coefficients for the membrane, the feed air boundary layer, and liquid desiccant boundary layer, respectively, each of which are defined in equations (7)-(9).

$$K_m = B/L \tag{7}$$

$$K_F = 0.0732\, Re^{0.6}\, Sc^{0.33}\, \frac{p}{p'}\frac{T'}{T}\frac{D}{d^{0.4}} \tag{8}$$

$$K_D \approx 0 \tag{9}$$

The expression for the membrane mass transfer coefficient K_m is obtained from the simple ratio of membrane vapor permeability B and thickness L. The air feed mass transfer coefficient K_F is given here by an empirical expression previously proposed for gas flow in hollow fiber membranes

[25-27], where *Re* is the Reynolds number, *Sc* is the Schmidt number, *D* is the diffusivity of water vapor, *d* is the hydraulic diameter, and p' and T' are standard pressure and temperature. And the mass transfer coefficient for the liquid desiccant is neglected $K_D \sim 0$, since the boundary layer gradient of water concentration is minimal [28].

2.3.Heat Transfer Across the Membrane

In a membrane-based dehumidification system, thermal energy transfer to the liquid desiccant solution is driven primarily by diffusion along a temperature gradient between the warm feed air and the cool liquid desiccant, as well as by vapor mass transfer that carries both latent and sensible heat across the membrane. When normalized per unit membrane surface area, the rate of thermal energy transfer can be expressed as heat flux $\dot{q}$.

$$\dot{q} = \frac{\Delta \dot{Q}}{a} = \dot{q}_{diffusion} + \dot{q}_{sensible} + \dot{q}_{latent} \tag{10a}$$

$$\dot{q} = \frac{\Delta \dot{Q}}{a} = \frac{\Delta T}{r} + J\, c_p\, T + J\, H_c \tag{10b}$$

Where $\dot{q}_{diffusion}$ is the temperature-driven thermal diffusion through the membrane, $\dot{q}_{sensible}$ is the heat carried by the water vapor mass that permeates across the membrane, and $\dot{q}_{latent}$ is the heat of condensation that is released from the water permeate phase change (which is assumed to occur only at the liquid desiccant surface). Expressions for each of these three thermal energy transfer mechanisms are provided in equation (10b), where ΔT is the temperature difference across the membrane and fluid boundary layers with thermal resistance *r*, c_p is the specific heat capacity, and H_c is the heat of condensation.

S. Moussaddy, S. Aryal, and J. Maisonneuve, "Specific energy analysis of using fertilizer-based liquid desiccants to dehumidify indoor plant environments," Applied Thermal Engineering (in press). https://doi.org/10.1016/j.applthermaleng.2023.121849

As stated previously, in cases where only an estimate of heat flux is needed, the temperatures and other fluid properties in equation (10) can be taken from the bulk fluids. However, to improve modelling accuracy, it is necessary to consider the non-linear temperature gradient across the fluid boundary layers, which will act to reduce heat flux (as well as mass flux).

In this case, a lumped element approach is taken and heat transfer across the membrane and the fluid boundary layers is considered. This is done by considering the temperature difference ΔT across each of their respective thermal resistances r. Where r_m, r_F, and r_D are thermal resistances for the membrane, the feed air boundary layer, and liquid desiccant boundary layer, respectively, each of which are defined in equations (11)-(13).

$$r_m = L/k \tag{11}$$

$$r_F = {h_F}^{-1} = \left(0.023 \frac{k}{d} Re^{0.8} Pr^{0.3}\right)^{-1} \tag{12}$$

$$r_D = {h_D}^{-1} = \left(0.36 \frac{k}{d} Re^{0.55} Pr^{0.33}\right)^{-1} \tag{13}$$

Where k is the thermal conductivity of either the membrane or the boundary layer fluid, h is the convection coefficient which is given here by empirical expressions previously proposed for shell and tube configurations [29, 30], and Pr is the Prandtl number for respective fluids.

3. Materials and Methods

3.1. Finite Element Analysis

A numerical approach was employed to evaluate the specific energy of dehumidification as a result of water vapor flux and heat flux in the fertilizer-based liquid desiccant system. A theoretical

model of mass and heat transport dynamics was developed using equations (1)-(14). The model was applied using discrete element analysis in 2-dimensions, including the direction normal to the membrane surface, and the direction axial to the membrane surface.

In the normal direction, concentration and temperature gradients develop due to different mass and thermal diffusivity rates across the membrane and its boundary layers. The normal profile was discretized into lumped elements, and a steady-state mass and energy balance was defined at both the air feed membrane surface and the liquid desiccant membrane surface. The governing equations of this balance are provided in Table 1, where the subscript *b* is used to define pressure and temperature of the bulk fluid, and subscript *m* is used to specify properties at the membrane surface.

Table 1. Steady state mass and energy balance at the membrane surfaces.

	Mass balance	Energy balance
Air feed membrane surface	$K_F\left(p_{H2O,F,b} - p_{H2O,F,m}\right) = K_m\left(p_{H2O,F,m} - p_{H2O,D,m}\right)$	$h_F\left(T_{F,b} - T_{F,m}\right) + J\, c_p\, T_{F,b} = \frac{k}{L}\left(T_{F,m} - T_{D,m}\right) + J\, c_p\, T_{F,m}$
Liquid desiccant membrane surface	$K_m\left(p_{H2O,F,m} - p_{H2O,D,m}\right) = K_D\left(p_{H2O,D,m} - p_{H2O,D,b}\right)$	$\frac{k}{L}\left(T_{F,m} - T_{D,m}\right) + J\, c_p\, T_{F,m} + J\, H_C = h_D\left(T_{D,m} - T_{D,b}\right) + J\, c_p\, T_{D,m}$

In the axial direction, concentration and temperature gradients develop due to the accumulation of water permeate and heat as the bulk liquid desiccant advances (and conversely the depletion of water permeate and heat from the bulk air feed). The axial profile was discretized into finite elements, and a steady-state mass and energy balance was defined for each element of bulk fluid

flow along the membrane surface. The governing equations of this balance are provided in Table 2.

Table 2. Steady state mass and energy balance for bulk air feed and liquid desiccant flow axial to the membrane surface.

	Mass balance	Energy balance
Air feed bulk fluid	$\dot{m}_{F,out} = \dot{m}_{F,in} - \Delta\dot{m}$	$\dot{Q}_{F,out} = \dot{Q}_{F,in} - \Delta\dot{Q}$
Liquid desiccant bulk fluid	$\dot{m}_{D,out} = \dot{m}_{D,in} + \Delta\dot{m}$	$\dot{Q}_{D,out} = \dot{Q}_{D,in} + \Delta\dot{Q}$

3.2. Numerical Methods

The mass and thermal transport model was implemented in Matlab software (R2018a, Mathworks, Natick, MA) and used to simulate the proposed dehumidification process. A numerical approach was employed to solve the system of equations. A complete logic of the model is provided is Figure 5. As shown, an iterative guess and check process is needed to consider polarization and solve for water vapor flux as a function of the membrane surface temperatures, which themselves are functions of vapor flux. In addition, an iterative loop is needed to march through discrete elements of the membrane length and account for axial variations in concentrations and temperatures by mass and energy balance. In the case where air feed is circulated counter to the liquid desiccant flow, the feed outlet conditions would need to be guessed and then iteratively corrected until the solution converges. However, this additional dynamic was neglected because in this study the liquid desiccant temperature and water concentration undergo only negligible axial variations along the length of the membrane, and therefore co-current modelling provides very similar results and is computationally simple.

S. Moussaddy, S. Aryal, and J. Maisonneuve, "Specific energy analysis of using fertilizer-based liquid desiccants to dehumidify indoor plant environments," Applied Thermal Engineering (in press). https://doi.org/10.1016/j.applthermaleng.2023.121849

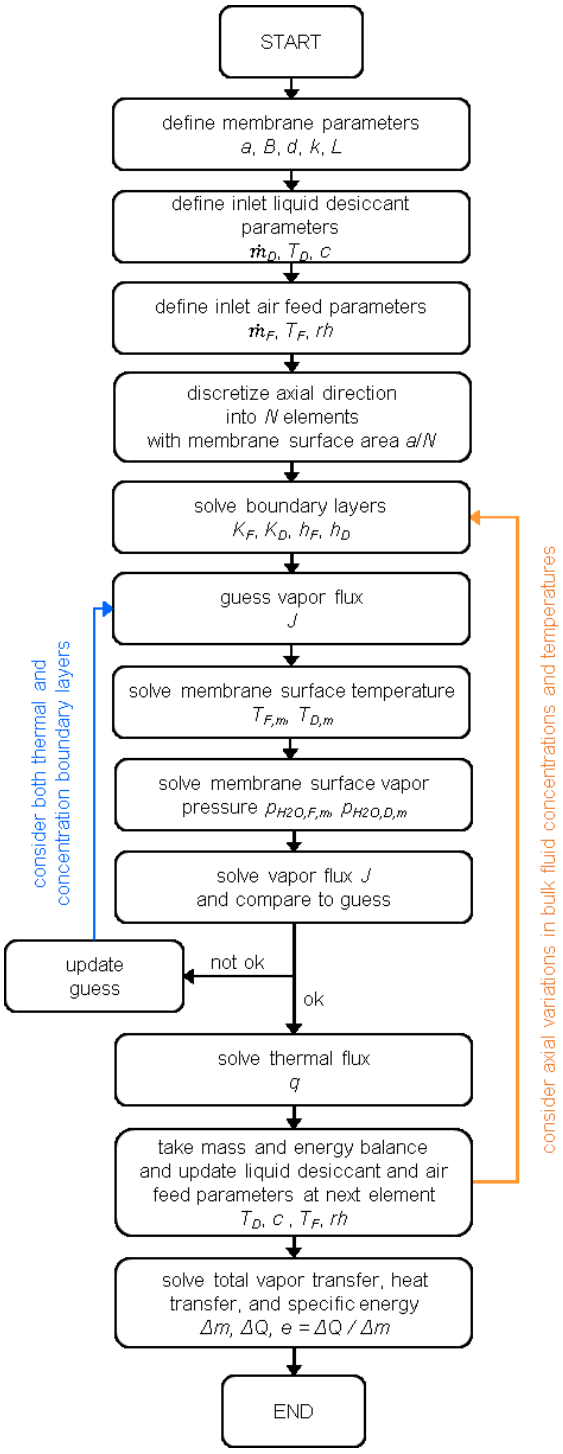

Figure 5. Finite element model used to numerically solve heat and mass transfer across each finite membrane element and determine the resulting energy and mass balance of each control volume throughout the liquid desiccant and air feed boundary layers.

S. Moussaddy, S. Aryal, and J. Maisonneuve, "Specific energy analysis of using fertilizer-based liquid desiccants to dehumidify indoor plant environments," Applied Thermal Engineering (in press). https://doi.org/10.1016/j.applthermaleng.2023.121849

3.3. Simulation Parameters

A number of different scenarios were simulated to evaluate performance, particularly the specific energy of dehumidification, over a range of operating and environmental conditions. A summary of the membrane characteristics and simulation input parameters is provided in Table 1. Unless otherwise specified, all results refer to these baseline conditions. The baseline is defined so as to be consistent with laboratory test conditions used in our previous study [22], and was experimentally validated as described in Section 3.4.. A hollow fiber module with a dense polydimethylsiloxane membrane was selected for the baseline scenario.

Table 3. Baseline simulation input parameters.

Membrane	
Configuration	hollow fiber
Material	polydimethylsiloxane
Vapor permeability B	3.94×10^{-6} g m^{-2} s^{-1} Pa^{-1}
Thermal conductivity k	0.19 W m^{-1} K^{-1} [31]
Membrane area a	1 m^2
Fiber thickness L	55×10^{-6} m
Fiber diameter d	300×10^{-6} m
Number of fibers	12,600
Shell channel diameter	6×10^{-2} m
Liquid Desiccant	
Flow direction	counter
Mass flow $\dot{m}$	2 lpm
Fertilizer solute	$Ca(NO_3)_2\,4H_2O$
Concentration c	945 g/l (75 % solubility)
Temperature T	15 °C

S. Moussaddy, S. Aryal, and J. Maisonneuve, "Specific energy analysis of using fertilizer-based liquid desiccants to dehumidify indoor plant environments," Applied Thermal Engineering (in press). https://doi.org/10.1016/j.applthermaleng.2023.121849

Coefficient of performance *COP*	5
Air Feed Supply	
Mass flow $\dot{m}$	5 slpm
Humidity *rh*	70 %
Temperature *T*	25 °C

3.4. Experimental Validation

Experimental validation of the mass and heat transport model was completed for baseline conditions using a laboratory test bench as shown in Figure 6. At the heart of the system is a commercial polydimethylsiloxane hollow fiber membrane module (PDMSXA-1.0, PermSelect, Ann Arbor MI).

Feed is circulated through the membrane fibers from a compressed air source. Air feed is heated and humidified to the target test conditions via an inline electric heater with a variable dc power source, and via bubbling through columns of deionized water. A mass and energy balance of the air feed is considered by measuring mass flow rate (GH-32907-69 mass flow controller, Masterflex, Radnor, PA), temperature in and out (MT-6340-30 thermal resistance sensors, TWTADE, Suzhou, China), and relative humidity in and out (AM2315 capacitive humidity sensors, Aosong Electronics, Guangzhou, China).

Liquid desiccant is pumped through the shell side of the membrane module from a reservoir of fertilizer solution prepared from deionized water and calcium nitrate tetrahydrate (98 % pure, Fisher-Scientific, Pittsburgh, PA). Liquid desiccant is cooled to the target temperature via circulation through a thermostatically controlled bath (TC550-SD, Brookfield, Middleboro, MA).

S. Moussaddy, S. Aryal, and J. Maisonneuve, "Specific energy analysis of using fertilizer-based liquid desiccants to dehumidify indoor plant environments," Applied Thermal Engineering (in press). https://doi.org/10.1016/j.applthermaleng.2023.121849

A mass and energy balance of the liquid desiccant is considered by measuring temperature in and out (800-32/140-1188 thermal resistance sensors, Noshok, Berea, OH).

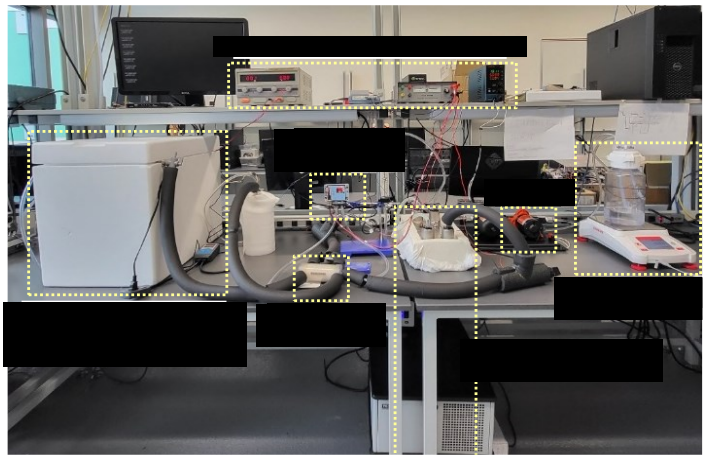

Figure 6. Liquid desiccant dehumidification test bench at Oakland University laboratory, used to experimentally validate the base case scenario defined in Table 3.

Figure 7 shows the water vapor and heat flux that are predicted by the transport model as well as the experimental observation of these from the experimental mass and energy balance. A significant level of consistency is observed between the results. Some degree of discrepancy is evident, but this may arise from inherent limitations within the chosen transport model correlations, as well as uncertainties inherent in the accuracy of the collected data. For reference, a complete data set is provided in Supplementary Notes 1 and 2, showing raw data, analysis, and propagation of uncertainty.

S. Moussaddy, S. Aryal, and J. Maisonneuve, "Specific energy analysis of using fertilizer-based liquid desiccants to dehumidify indoor plant environments," Applied Thermal Engineering (in press). https://doi.org/10.1016/j.applthermaleng.2023.121849

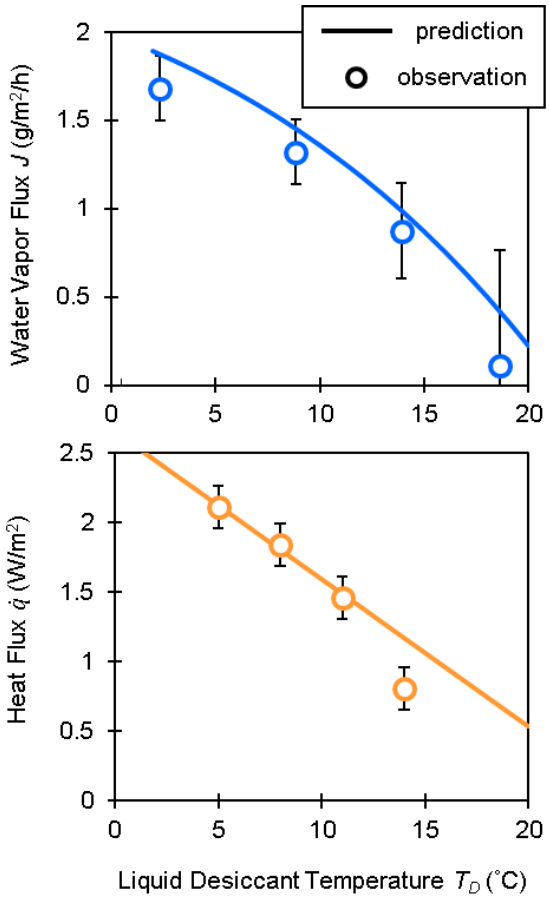

Figure 7. Water vapor flux and heat flux as predicted by the transport model and as observed by laboratory testing under base case conditions defined in Table 3.

4. Results

4.1. Specific Energy of Dehumidification

Figure 8 shows the specific energy results for fertilizer-based dehumidification given the base case conditions previously specified in Table 3. As shown, water vapor flux increases significantly as liquid desiccant solution is cooled, and simultaneously, a significant increase in heat flux is observed. For example, vapor flux increases from 0.2 to 1.3 g/m^2/h as desiccant temperature is halved from 20 to 10 °C, but heat flux also increases from 0.55 to 1.65 W/m^2. The balance of these

two competing dynamics is observed in the specific energy of dehumidification, where a minimum of 0.24 Wh/g is achieved at 13 °C, assuming the cooling load can be handled with a coefficient of performance COP = 5. The effect of higher or lower COP is also shown. These specific energy results compare favorably against both the thermodynamic limit of dehumidification which is 0.14 Wh/g for this case, and the new California greenhouse standards which range from 0.37 to 0.55 Wh/g.

S. Moussaddy, S. Aryal, and J. Maisonneuve, "Specific energy analysis of using fertilizer-based liquid desiccants to dehumidify indoor plant environments," Applied Thermal Engineering (in press). https://doi.org/10.1016/j.applthermaleng.2023.121849

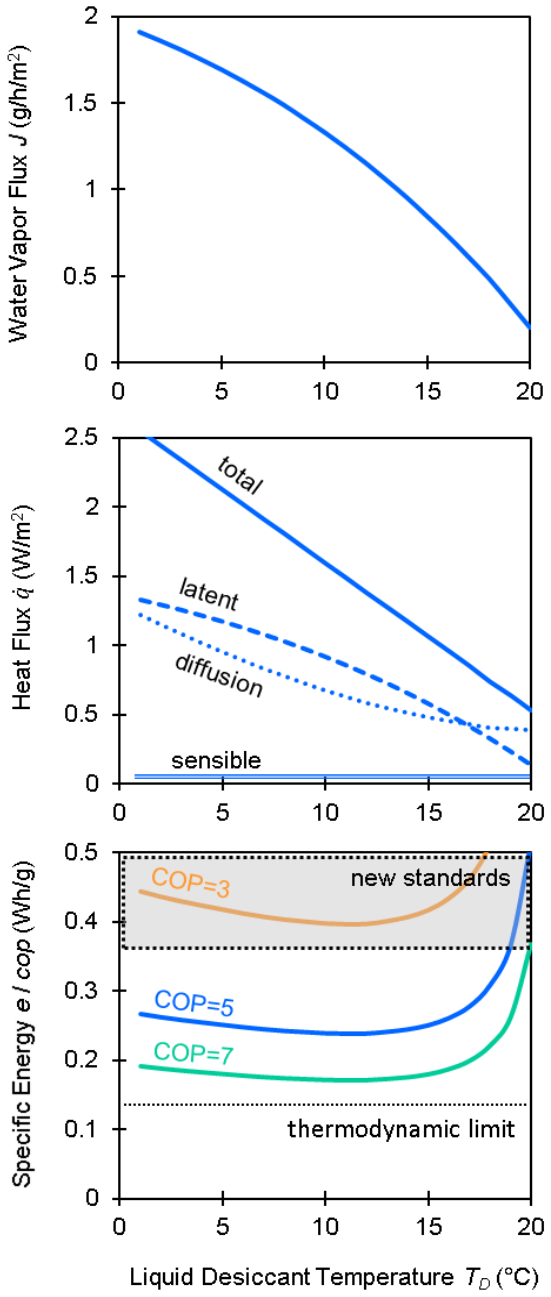

Figure 8. Water vapor and heat flux received by a fertilizer-based liquid desiccant solution across a range of desiccant temperatures. Specific energy of dehumidification is obtained from the ratio of heat flux to vapor flux, and normalized over the assumed coefficient of performance of the cooling technology (i.e. e / COP). The thermodynamic limit of dehumidification, and new energy efficiency standards are provided for reference. Unless otherwise specified, default simulation parameters are specified in Table 3.

S. Moussaddy, S. Aryal, and J. Maisonneuve, "Specific energy analysis of using fertilizer-based liquid desiccants to dehumidify indoor plant environments," Applied Thermal Engineering (in press). https://doi.org/10.1016/j.applthermaleng.2023.121849

As shown, total heat flux is linearly proportional to the liquid desiccant temperature. A linear profile like this is characteristic of a heat transfer process that is approaching thermal equilibrium. In this case, the air feed has low thermal capacity (relative to that of the liquid desiccant), and the membrane is somewhat oversized (relative to the feed flow rate) providing ample surface area for heat transfer. Under these conditions, air feed leaves the membrane module at temperatures approximately equal to the liquid desiccant inlet. This is confirmed by reviewing the raw data, such as provided in Supplementary Notes 1 and 2, which shows that $T_{F,out} \rightarrow T_{D,in}$. The total heat flux curve is therefore only a representation of the thermal equilibrium limit, which is a linear function of the liquid desiccant temperature. Figure 8 also shows the relative contribution of different heat transfer mechanisms to the total flux. These mechanisms include (1) diffusion of heat across the membrane (dotted line), (2) latent heat released from condensation of vapor permeate (hatched line), and (3) sensible heat carried by the vapor mass transfer (double line). The third mechanism of sensible heat transfer is shown to be negligible, and therefore it is not included in further analysis. The second mechanism of latent heat transfer by condensation is of course proportional to the rate of vapor mass transfer, and as shown the latent heat flux curve follows the vapor flux curve. Interestingly, any change in latent heat flux is countered by an opposite change in thermal diffusion which establishes thermal equilibrium and generates the linear plot for total flux that is explained above.

4.2.Liquid Desiccant Dilution

One of the primary features of fertilizer-based liquid desiccant is that, unlike conventional desiccant, its concentration is not maintained via an energy intensive heating and cooling

regeneration cycle. Instead, a batch of fertilizer desiccant is recirculated through the membrane dehumidification system, recovering water vapor from the indoor plant environment, until the solution is sufficiently diluted for delivery to the plants. However, as the concentration of desiccant drops, so does its dehumidification potential. The transient nature of this process has an important effect on its energy efficiency, as well as on its ability to match plant evapotranspiration rates, which are also highly dynamic.

Figure 9 shows water vapor flux and the resulting specific energy of dehumidification, as fertilizer concentration is diluted from near the solubility limit down to 10 % and then 0.1 % solubility. Such low concentrations are on the order of what is typically desired for safe delivery of fertilizers to plants. For example, in the case of $Ca(NO_3)_2$ which is selected for this study, it is typically delivered to plants at concentrations of ~ 1 g/l, equivalent to ~ 0.1 % of solubility [32].

As expected, vapor flux drops as solution is diluted, and the resulting specific energy of dehumidification increases. In addition, we observe that the minimum specific energy point shifts to lower temperatures at low concentrations. This suggests the need to progressively cool the fertilizer solution, as the batch process advances and the solution is diluted. To illustrate, consider the case where fertilizer solution is maintained at a constant 13 °C as it is diluted. In this case, water vapor flux would drop from 1.12 to 0.86 g/m^2/h, and as a result the specific energy would increase from 0.23 to 0.30 Wh/g. If however, the fertilizer temperature is progressively reduced from 13 to 10 °C as the solution is diluted, vapor transfer would be maintained at a nearly constant rate, and the specific energy would only increase from 0.23 to 0.27 Wh/g.

Interestingly, total heat flux remains constant across all the different concentrations. This may appear to be somewhat counter intuitive since latent heat transfer by condensation is proportional

to the rate of vapor mass transfer, which drops as desiccant concentration is reduced. However, we observe here that any drop in the latent heat of condensation is followed by an equal and opposite increase in thermal diffusion, such that total flux will remain constant. This is because the process is operating near its thermal equilibrium limit, as explained in Section 4.1. Under these conditions, thermal diffusion can be quite significant. This is well illustrated in Figure 9 at temperatures of around 20 °C, where even in the absence of condensation, when mass transfer is reduced to zero due to low concentration desiccant, thermal equilibrium is established by diffusion alone and total flux remains constant.

S. Moussaddy, S. Aryal, and J. Maisonneuve, "Specific energy analysis of using fertilizer-based liquid desiccants to dehumidify indoor plant environments," Applied Thermal Engineering (in press). https://doi.org/10.1016/j.applthermaleng.2023.121849

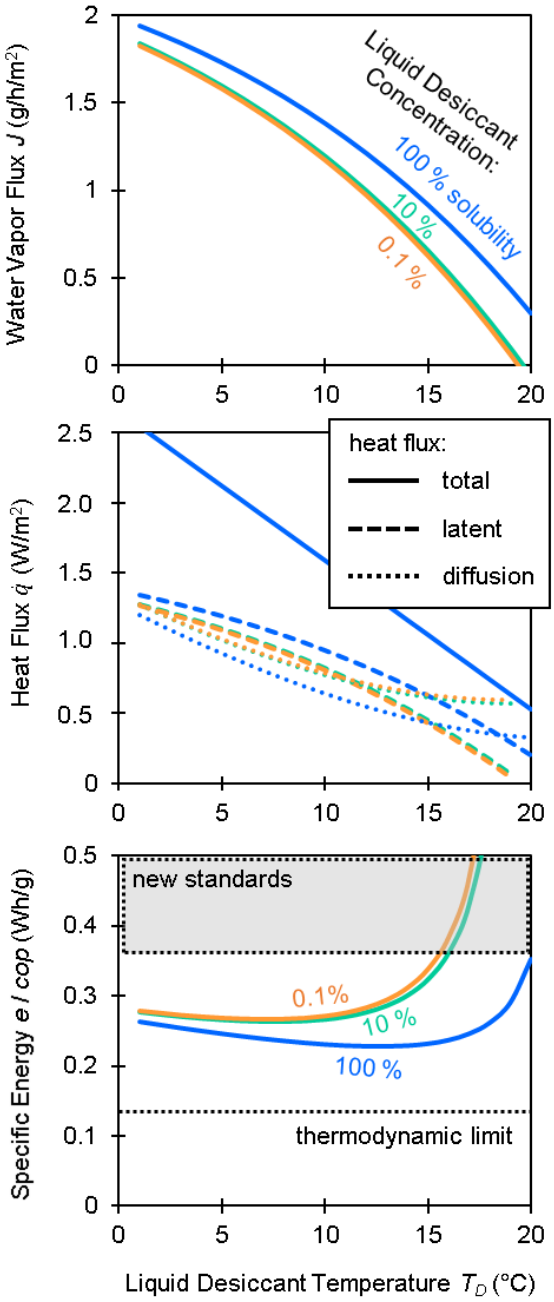

Figure 9. Water vapor and heat flux received by a fertilizer-based liquid desiccant solution across a range of fertilizer solution concentrations. Specific energy of dehumidification is obtained from the ratio of heat flux to vapor flux, and normalized over the coefficient of performance of the cooling technology (i.e. *e* / *COP*). The thermodynamic limit of dehumidification, and new energy efficiency standards are provided for reference. Unless otherwise specified, default simulation parameters are specified in Table 3.

S. Moussaddy, S. Aryal, and J. Maisonneuve, "Specific energy analysis of using fertilizer-based liquid desiccants to dehumidify indoor plant environments," Applied Thermal Engineering (in press). https://doi.org/10.1016/j.applthermaleng.2023.121849

4.3.Liquid Desiccant and Air Feed Circulation Rates

Performance of the proposed fertilizer-based dehumidification system can be optimized by careful control of operating conditions, including the circulation rates of liquid desiccant and air feed. For example, axial gradients of temperature and concentration can be mitigated by reducing the residence time of fluids in the membrane system. In addition, boundary layers and their associated transport resistances can be reduced by maintaining high velocities and high Reynolds numbers.

Figure 10 shows the effect that different circulation rates have on dehumidification performance. As shown, a small improvement in vapor flux is noted from higher liquid desiccant circulation rates. This is driven by a reduction in concentration polarization due to improved mixing that occurs at higher Reynolds numbers. There is no observed effect on heat flux, because again the circulating air reaches thermal equilibrium with the liquid desiccant temperature, and any difference in heat of condensation is only offset by more or less diffusion.

A more important change in performance is observed in response to different air circulation rates. Performance is much more sensitive to air circulation because air temperatures vary over the surface of the membrane before converging towards the liquid desiccant temperature at thermal equilibrium. Greater circulation rates for the air feed allow it to maintain relatively stable temperatures over a greater portion of the membrane surface, thereby improving flux, but conversely this also means that a greater mass of air is cooled to the liquid desiccant equilibrium temperature, which represents more thermal energy transfer. For example, an increase in air circulation rates from 1 to 10 lpm is shown to cause an increase in vapor and heat flux from 0.34 to 1.31 g/ m^2/h and 0.25 to 2.55 W/m^2, respectively (at liquid desiccant temperatures of 13 °C).

S. Moussaddy, S. Aryal, and J. Maisonneuve, "Specific energy analysis of using fertilizer-based liquid desiccants to dehumidify indoor plant environments," Applied Thermal Engineering (in press). https://doi.org/10.1016/j.applthermaleng.2023.121849

This particular tradeoff is unfavorable, and from among the cases considered, the lowest specific energy results are obtained at low air flow rates of 1 lpm, in which case very impressive results as low as 0.15 Wh/g are predicted.

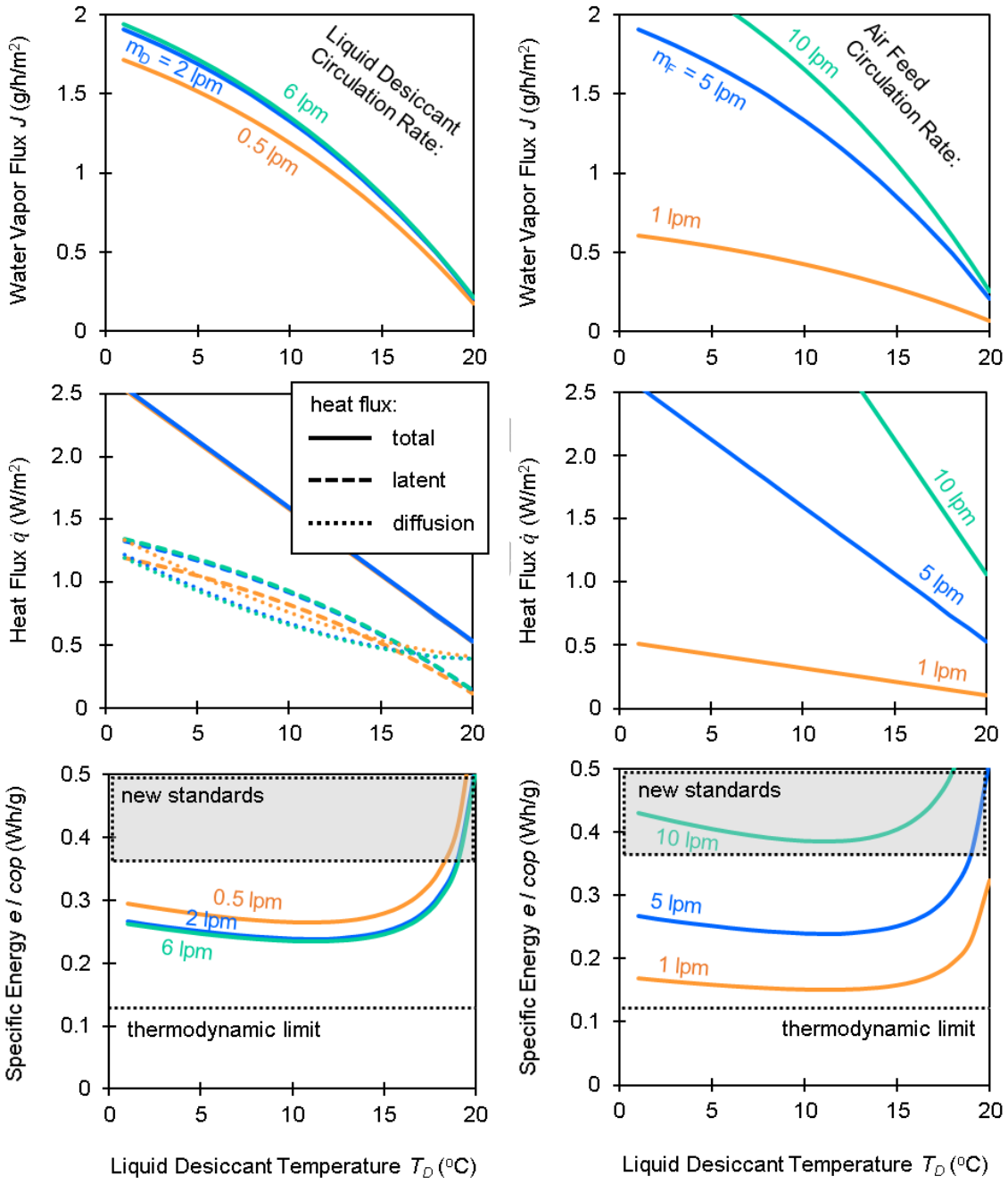

S. Moussaddy, S. Aryal, and J. Maisonneuve, "Specific energy analysis of using fertilizer-based liquid desiccants to dehumidify indoor plant environments," Applied Thermal Engineering (in press). https://doi.org/10.1016/j.applthermaleng.2023.121849

Figure 10. Water vapor and heat flux received by a fertilizer-based liquid desiccant solution across a range of circulation rates for both the liquid desiccant and the air feed. Specific energy of dehumidification is obtained from the ratio of heat flux to vapor flux, and normalized over the coefficient of performance of the cooling technology (i.e. e / COP). The thermodynamic limit of dehumidification, and new energy efficiency standards are provided for reference. Unless otherwise specified, default simulation parameters are specified in Table 3.

These results indicate the need to optimize operating parameters including the air feed and liquid desiccant circulation rates. Low circulation rates were favored here, but the conditions for minimum specific energy will be highly case specific and scaled proportionate to the membrane surface area and channel geometry. Importantly, we do not consider here the effect of friction losses, which would impose an energy penalty for high circulation rates. This would need to be considered in further optimization.

4.4.High Performance Membranes

Fertilizer-based liquid desiccants can be applied in a number of desiccant systems (such as spray dehumidification and evaporative coolers) but in this study a membrane dehumidification system is featured [33,34]. As a result, membrane selection will be a significant factor in the performance of the dehumidification system. Ideally, a membrane will exhibit very high water vapor permeability to encourage dehumidification mass transfer, but very low thermal conductivity so as to minimize the desiccant cooling load by mitigating thermal diffusion [35].

Figure 11 shows dehumidification for a selection of three different membrane materials. Performance of the default polydimethylsiloxane (PDMS) membrane is compared against a high permeability polyether block amide (PEBAX) membrane, and a low permeability polyether sulfone (PES) membrane. As shown, the membrane's vapor permeability has a significant impact

on performance. This is clear from the large difference in vapor flux that is observed for the different membranes. To illustrate, consider operation at 15 °C where vapor flux increases from 0.85 g/m^2/h for PDMS to 1.30 g/m^2/h for PEBAX, and as a result the specific energy reduces from 0.25 to 0.16 Wh/g. This approaches the thermodynamic limit of dehumidification. Moreover, the specific energy profile of PEBAX appears to be relatively stable over a range of liquid desiccant temperatures ranging from approximately 5 to 15 °C. This can provide some advantages and operational flexibility for controlling a future dehumidification prototype that will need to balance dehumidification efficiency and dehumidification rate.

S. Moussaddy, S. Aryal, and J. Maisonneuve, "Specific energy analysis of using fertilizer-based liquid desiccants to dehumidify indoor plant environments," Applied Thermal Engineering (in press). https://doi.org/10.1016/j.applthermaleng.2023.121849

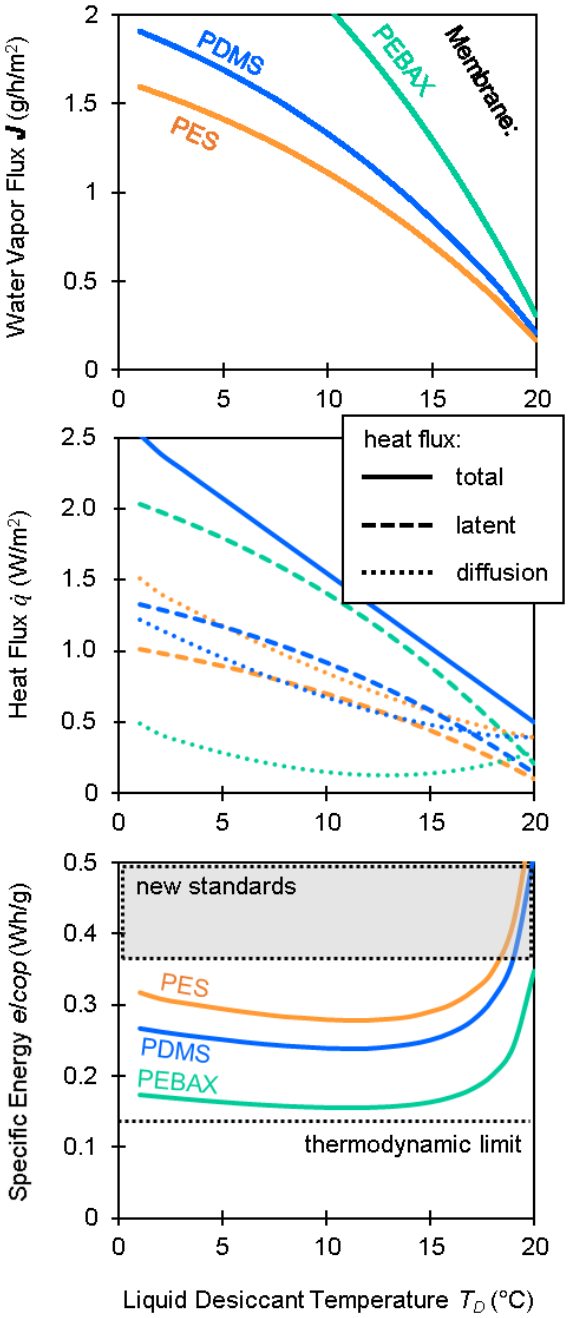

Figure 11. Water vapor and heat flux received by a fertilizer-based liquid desiccant solution across a selection of different membranes. Polyether block amide (PEBAX) has vapor permeability $B = 5.48 \times 10^{-6}$ g m^{-2} s^{-1} Pa^{-1} [36]. Polydimethylsiloxane (PDMS) has vapor permeability $B = 3.94 \times 10^{-6}$ g m^{-2} s^{-1} Pa^{-1} [31]. Polyether sulfone (PES) has vapor permeability $B = 0.49 \times 10^{-6}$ g m^{-2} s^{-1} Pa^{-1} [37-38]. All other default simulation parameters are specified in Table 3.

S. Moussaddy, S. Aryal, and J. Maisonneuve, "Specific energy analysis of using fertilizer-based liquid desiccants to dehumidify indoor plant environments," Applied Thermal Engineering (in press). https://doi.org/10.1016/j.applthermaleng.2023.121849

5. Conclusions

This study evaluates the performance and energy efficiency of using fertilizer-based liquid desiccants for dehumidification of indoor plant environments. The novel fertilizer concept is applied here to a membrane-based dehumidification process that has been modeled and experimentally validated. Performance is simulated across a range of operating conditions, with particular consideration for the liquid desiccant temperature. Other variables include the liquid desiccant concentration, the liquid desiccant and air feed circulation rates, and the membrane material. Mass and heat transfer are accounted for and energy efficiency is evaluated in terms of the specific energy of dehumidification, which is the ratio of the water vapor removed from the air versus the heat that is transferred to the cool liquid desiccant (which must then be rejected from the system via a cooling unit with some coefficient of performance).

Specific energy was found to be highly dependent on liquid desiccant temperature. At lower desiccant temperatures, desiccant vapor pressure is reduced and hence additional vapor transfer is promoted. However, cooling the liquid desiccant also drives additional heat transfer from the warm feed air. This tradeoff is clearly illustrated throughout the results, and there is shown to be an optimal liquid desiccant temperature that will maximize the ratio of vapor removal to heat transfer, thereby minimizing the specific energy of dehumidification. Minimum specific energy between 0.16-0.24 Wh/g was achieved across the various cases studied. This compares very favorably with the thermodynamic limit of enthalpy of condensation of 0.14 Wh/g. It also compares favorably with other dehumidification technologies available on the market [19], and satisfies new energy efficiency standards for indoor plant cultivation which require between 0.37-0.55 Wh/g [20, 21].

S. Moussaddy, S. Aryal, and J. Maisonneuve, "Specific energy analysis of using fertilizer-based liquid desiccants to dehumidify indoor plant environments," Applied Thermal Engineering (in press). https://doi.org/10.1016/j.applthermaleng.2023.121849

Across the range of parameters considered, the liquid desiccant temperature for the minimum specific energy appeared between 7-14 °C, but it is highly case specific. For example, at different fertilizer concentrations, the minimum specific energy was achieved at different liquid desiccant temperatures. In general, lower fertilizer concentration leads to decreased vapor flux and increased specific energy use, and the minimum specific energy point is shifted to a lower desiccant temperature. This suggests that liquid desiccant temperature should be actively controlled throughout a fertilizer dehumidification batch process, because as water vapor is removed from the air and accumulated by the liquid desiccant, the fertilizer concentration will reduce in real time. Active control of liquid desiccant temperature could be done to (i) ensure efficient operation at the minimum specific energy point, and (ii) ensure vapor removal rates are sufficient to maintain target greenhouse conditions. Such dynamic control would need to account for not only changes in the liquid desiccant concentration (which is diluted over time), but also for changes in the environmental conditions (as the rates of plant evapotranspiration are expected to vary throughout the day and throughout the plant lifecycle). Such active control strategies should be considered in future work.

Vapor flux associated with operation at the minimum specific energy points ranged from 1.2-1.6 g/m^2/h. These vapor removal rates are relatively modest and other membrane-based desiccant studies have reported much higher flux [39,40]. However, lower vapor flux is somewhat to be expected in this study because membrane surface area is somewhat oversized relative to the air feed circulation rates. Other studies that used similar amounts of membrane area relative to feed circulation, have obtained similar vapor flux as reported here [41]. This dynamic is clearly illustrated in the analysis of the air feed circulation rates, which showed much better vapor flux when air feed flow rates were increased. Vapor flux is an important metric because it provides an

indicator of the amount of membrane area, and hence capital, that would be required to scale up the system and achieve a certain target dehumidification capacity as required by the greenhouse.

Other variables considered in this study included the liquid desiccant circulation rate and the membrane material. Changes in the liquid desiccant circulation rates had only a minor effect on performance. This suggests that the liquid desiccant circulation rates are excessive and should be optimized in proportion to the membrane surface area and geometry. For the membrane material, PEBAX outperformed PDMS and PES in terms of both vapor flux and specific energy. These findings established that materials with higher vapor permeability enabled greater water vapor transfer, consequently reducing the specific energy required for dehumidification.

In conclusion, this work contributes to the literature by providing the first ever specific energy analysis of using fertilizer-based liquid desiccants for dehumidification. The results are encouraging and justify further research and development of the concept. In particular, we recommend future work to prototype the technology and integrate the proposed real-time control of liquid desiccant temperature.

Acknowledgements

This material is based upon work supported by the National Science Foundation, award number 2301488.

Nomenclature

a	membrane surface area (m^2)
B	vapor permeability ($g\ m^{-2}\ s^{-1}\ Pa^{-1}$)
c	concentration ($mol\ l^{-1}$)
COP	coefficient of performance

S. Moussaddy, S. Aryal, and J. Maisonneuve, "Specific energy analysis of using fertilizer-based liquid desiccants to dehumidify indoor plant environments," Applied Thermal Engineering (in press). https://doi.org/10.1016/j.applthermaleng.2023.121849

c_p	specific heat (J K^{-1} g^{-1})
D	diffusivity (m^2 s^{-1})
d	diameter (m)
e	specific energy (kWh/kg)
H_c	heat of condensation (J g^{-1})
h	heat transfer coefficient (W m^{-2} K^{-1})
i	number of ions
J	vapor flux (g m^{-2} s^{-1})
K	mass transfer coefficient (g m^{-2} s^{-1} Pa^{-1})
k	thermal conductivity (W m^{-1} K^{-1})
L	membrane thickness (m)
m	mass (g)
Pr	Prandtl number
p	pressure (Pa)
$\dot{Q}$	heat transfer rate (W)
$\dot{q}$	heat flux (W m^{-2})
R	gas constant (J mol^{-1} K^{-1})
Re	Reynolds number
r	thermal resistance (K m^2 W^{-1})
rh	relative humidity (%)
Sc	Schmidt number
T	temperature (K)
V_m	molar volume (m^3 mol^{-1})
W	work (J)
x	mole fraction

Greek symbols:

π	osmotic pressure (Pa)

Subscripts and Superscripts:

b	bulk fluid
D	liquid desiccant

S. Moussaddy, S. Aryal, and J. Maisonneuve, "Specific energy analysis of using fertilizer-based liquid desiccants to dehumidify indoor plant environments," Applied Thermal Engineering (in press). https://doi.org/10.1016/j.applthermaleng.2023.121849

F	air feed
H2O	water / vapor
in	membrane module inlet
m	membrane surface
o	reference or standard conditions
out	membrane module outlet

References

[1] J.R. Schramski, C.B. Woodson, and J.H. Brown, "Energy use and the sustainability of intensifying food production," *Nature Sustainability*, vol. 3, pp. 257–259, 2020.

[2] C. Stanghellini, "Horticultural production in greenhouses: Efficient use of water," *Acta Horticulturae*, vol. 1034, pp. 25-32, 2014.

[3] P. Padmanabhan, A. Cheema, and G. Paliyath, "Encyclopedia of Food and Health," Academic Press, pp. 24–32, 2016.

[4] A. Vadiee and V. Martin, "Energy management strategies for commercial greenhouses," *Applied Energy*, vol. 114, pp. 880-888, 2014.

[5] A. Vadiee and V. Martin, "Energy management in horticultural applications through the closed greenhouse concept, state of the art," *Renewable and Sustainable Energy Reviews*, vol. 16 (7), pp. 5087-5100, 2012.

[6] T. Qian, J. Dieleman, A. Elings, G. Arie, L.F.M. Marcelis, and O. Kooten, "Comparison of climate and production in closed, semi-closed and open greenhouses," *Acta Horticulturae*, vol. 893, 2009.

S. Moussaddy, S. Aryal, and J. Maisonneuve, "Specific energy analysis of using fertilizer-based liquid desiccants to dehumidify indoor plant environments," Applied Thermal Engineering (in press). https://doi.org/10.1016/j.applthermaleng.2023.121849

[7] L.D. Albright et al, "An air-liquid-air heat exchanger for greenhouse humidity control," *Transactions of the American Society of Agricultural Engineers*, vol.27, 1986.

[8] N. Katsoulas et al, "Reducing ventilation requirements in semi-closed greenhouses increases water use efficiency," *Agricultural Water Management*, vol. 156, 2015.

[9] G.A. Longo and A. Gasparella, "Experimental and theoretical analysis of heat and mass transfer in a packed column dehumidifier/regenerator with liquid desiccant," *International Journal of Heat and Mass Transfer*, vol 48 (25), pp. 5240-5254, 2005.

[10] A. Lowenstein, "Review of Liquid Desiccant Technology for HVAC Applications," *HVAC&R Research*, vol.14 (6), pp. 819-839, 2008

[11] X. Niu, F. Xiao, and Z.Ma, "Investigation on capacity matching in liquid desiccant and heat pump hybrid air-conditioning systems," *International Journal of Refrigeration*, vol 35, pp. 160-170, 2012.

[12] A. Ali, K. Ishaque, A. Lashin, and N. Al Arifi, "Modeling of a liquid desiccant dehumidification system for close type greenhouse cultivation," *Energy*, vol. 118, pp. 578-589, 2017.

[13] X. Liu, M. Qu, X. Liu, and L. Wang, "Membrane-based liquid desiccant air dehumidification: A comprehensive review on materials, components, systems and performances," *Renewable and Sustainable Energy Reviews*, vol. 110, pp. 444-466, 2019.

S. Moussaddy, S. Aryal, and J. Maisonneuve, "Specific energy analysis of using fertilizer-based liquid desiccants to dehumidify indoor plant environments," Applied Thermal Engineering (in press). https://doi.org/10.1016/j.applthermaleng.2023.121849

[14] J.L. Niu and L.Z. Zhang, "Membrane-based enthalpy exchanger: material considerations and clarification of moisture resistance," *Journal of Membrane Science*, vol. 189 (2), pp. 179–191, 2001.

[15] R. S. Das, and S. Jain, "Performance characteristics of cross-flow membrane contactors for liquid desiccant systems," *Applied Energy*, vol. 141, pp. 1-11, 2015.

[16] C. Tang, K. Vafai, C. Gu, K. N. Gloria, and M.D. Razaul Karim, "Experimental investigation of dehumidification performance of a vapor compression refrigeration system," *International Communications in Heat and Mass Transfer*, vol. 137, 106282, 2022.

[17] R. Lefers, N.M.S. Bettahalli, S. Nunes, N.V. Fedoroff, P.A. Davies, and T. Leiknes, "Liquid desiccant dehumidification and regeneration process to meet cooling and freshwater needs of desert greenhouses," *Desalination and Water Treatment*, vol. 57, pp. 23430–23442, 2016.

[18] N. Zhang, S.-Y. Yin, and M. Li, "Model-based optimization for a heat pump driven and hollow fiber membrane hybrid two-stage liquid desiccant air dehumidification system," *Applied Energy*, vol. 228, pp. 12-20, 2018.

[19] Yang, K.-S., Wang, J.-S., Wu, S.-K., Tseng, C.-Y., and Shyu, J.-C. "Performance evaluation of a desiccant dehumidifier with a heat recovery unit," *Energies*, vol. 10(12), 2017.

[20] M. Amani, S. Foroushani, M. Sultan, and M. Bahrami, "Comprehensive review on dehumidification strategies for agricultural greenhouse applications," Applied Thermal Engineering, vol. 181, page 115979, 2020.

S. Moussaddy, S. Aryal, and J. Maisonneuve, "Specific energy analysis of using fertilizer-based liquid desiccants to dehumidify indoor plant environments," Applied Thermal Engineering (in press). https://doi.org/10.1016/j.applthermaleng.2023.121849

[21] Energy Solutions and Cultivate Energy and Optimization, "Codes and Standards Enhancement (CASE) Initiative 2022 California Energy Code," March 2022.

[22] S. Moussaddy, S. Pushparajah, and J. Maisonneuve, "Fertilizer-Based Liquid Desiccants: A Novel Concept for Energy Efficient Dehumidification and Water Vapor Recycling in Indoor Plant Environments," *Applied Thermal Engineering*, vol. 219 Part B, 119529, 2022.

[23] J. Lee and R. Karnik, "Desalination of water by vapor-phase transport through hydrophobic nanopores," *Journal of Applied Physics*, vol. 108, 044315, 2010.

[24] J. Lee, A. P. Straub, and M. Elimelech, "Vapor-gap membranes for highly selective osmotically driven desalination," Journal of Membrane Science, vol. 555, pp. 407-417, 2018.

[25] G. He, Y. Mi, P. Lock Yue, and G. Chen. "Theoretical study on concentration polarization in gas separation membrane processes," *Journal of Membrane Science*, vol. 153, pp. 243-258, 1999.

[26] S. Moussaddy, G. Yuan, and J. Maisonneuve, "A new concept for generating mechanical work from gas permeation," *Journal of Membrane Science*, vol. 614 (118489), 2020.

[27] S. Moussaddy and J. Maisonneuve, "Energy from carbon dioxide: Experimental and theoretical analysis of power generation from membrane-based sweep gas permeation," *Journal of Membrane Science*, vol. 644 (120053), 2022.

[28] V. Karanikola et al., "Sweeping gas membrane distillation: Numerical simulation of mass and heat transfer in a hollow fiber membrane module," Journal of Membrane Science, vol. 483, pp. 15–24, 2015.

S. Moussaddy, S. Aryal, and J. Maisonneuve, "Specific energy analysis of using fertilizer-based liquid desiccants to dehumidify indoor plant environments," Applied Thermal Engineering (in press). https://doi.org/10.1016/j.applthermaleng.2023.121849

[29] S.W.L. Alan, M.R. Islam, and K.J. Chua, "A Theoretical Model on Internally Cooled Liquid Desiccant Dehumidification and Cooling Processes," *Energy Procedia*, vol. 142, pp. 1009-1014, 2017.

[30] W. Roetzel, X. Luo, and D. Chen, "Design and Operation of Heat Exchangers and their Networks," *Academic Press*, 2020.

[31] E. E. Matula and J. A. Nabity, "Characterization of simultaneous heat, oxygen, and carbon dioxide transfer across a nonporous polydimethylsiloxane (PDMS) hollow fiber membrane," *Chemical Engineering Journal Advances,* vol. 6 (100106), 2021.

[32] P. Pourmovahed, M. Lefsrud, and J. Maisonneuve, "Thermodynamic limits of using fertilizer to produce clean fertigation solution from wastewater via forward osmosis," *Journal of Membrane Science*, vol. 647 (120168), 2021.

[33] S. Gumruk, M. K. Aktas, and F. Kasap, "Experimental investigation of spray dehumidification process in moist air," *International Communications in Heat and Mass Transfer*, vol. 97, pp. 163–171, 2018.

[34] N. Kapilan, A. M. Isloor, and S. Karinka, "A comprehensive review on evaporative cooling systems," *Results in Engineering*, vol. 18, p. 101059, 2023.

[35] Z-X Li and L-Z. Zhang, "Flow maldistribution and performance deteriorations in a counter flow hollow fiber membrane module for air humidification/dehumidification," *International Journal of Heat and Mass Transfer*, vol. 74, pp. 421-430, 2014.

S. Moussaddy, S. Aryal, and J. Maisonneuve, "Specific energy analysis of using fertilizer-based liquid desiccants to dehumidify indoor plant environments," Applied Thermal Engineering (in press). https://doi.org/10.1016/j.applthermaleng.2023.121849

[36] F. H. Akhtar, M. Kumar, and K.-V. Peinemann, "Pebax®1657/Graphene oxide composite membranes for improved water vapor separation," *Journal of Membrane Science*, vol. 525, pp. 187-194, 2017.

[37] P. G. Ingole, M. Sohail, A. M. Abou-Elanwar, M. I. Baig, J.-D. Jeon, W. K. Choi, H. Kim, and H. K. Lee, "Water vapor separation from flue gas using MOF incorporated thin film nanocomposite hollow fiber membranes", *Chemical Engineering Journal*, vol. 334, pp. 2450-2458, 2018.

[38] S. J. Metz, W. J. C. van de Ven, J. Potreck, M. H. V. Mulder, and M. Wessling, "Transport of water vapor and inert gas mixtures through highly selective and highly permeable polymer membranes," *Journal of Membrane Science*, vol. 251(1-2), pp. 29-41, 2005.

[39] M Huang, M. Yang, and X. Yang, "Performance analysis of a quasi-counter flow parallel-plate membrane contactor used for liquid desiccant air dehumidification," *Applied Thermal Engineering,* vol. 63, pp. 323–332, 2014.

[40] X. Chen, Y. Su, D. Aydin, H. Bai, H. Jarimi, X. Zhang, and S. Riffat, "Experimental investigation of a polymer hollow fibre integrated liquid desiccant dehumidification system with aqueous potassium formate solution," *Applied Thermal Engineering*, vol. 142, pp. 632-643, 2018.

[41] X. Liu, J. Warner , M. Qu, X. Liu, and H. Opadrishta, "A Preliminary Experimental Study on the Performance of a Membrane-based Air Dehumidifier Using Ionic Liquid," in *International Refrigeration and Air Conditioning Conference*, Purdue University, West Lafayette, IN, vol. 2081, pp. 1-10, 2018.

S. Moussaddy, S. Aryal, and J. Maisonneuve, "Specific energy analysis of using fertilizer-based liquid desiccants to dehumidify indoor plant environments," Applied Thermal Engineering (in press). https://doi.org/10.1016/j.applthermaleng.2023.121849

SUPPLEMENTARY INFORMATION

Supplementary Note 1: Sample Test Data, Analytical Methods, and Uncertainty Analysis for Validation of the Vapor Transport Model

The proposed mass transport model was validated using a series of tests performed on the Oakland University laboratory bench. Figure S1 shows raw data collected for a sample test trial, and Table S1 provides a detailed outline of how data is analyzed, including how experimental uncertainty is propagated throughout the analysis. Vapor flux was evaluated by considering a mass balance of the air feed.

(a) Air feed flow rate as measured by mass flow controller (GH-32907-69, Masterflex, Radnor, PA).

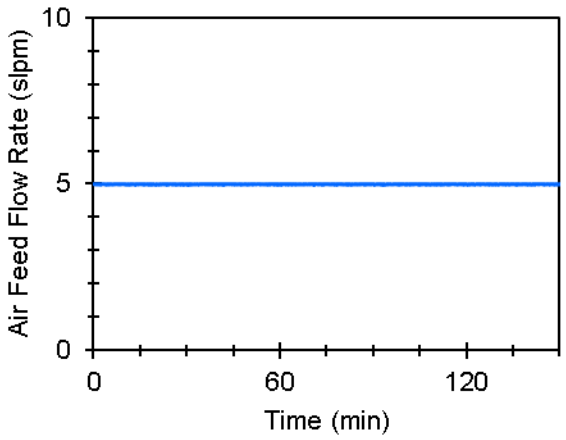

(b) Air feed relative humidity (at specified temperature) at the inlet and outlet as measured by temperature and humidity sensors (AM2315 i2C, Aosong, Guangzhou, China).

S. Moussaddy, S. Aryal, and J. Maisonneuve, "Specific energy analysis of using fertilizer-based liquid desiccants to dehumidify indoor plant environments," Applied Thermal Engineering (in press). https://doi.org/10.1016/j.applthermaleng.2023.121849

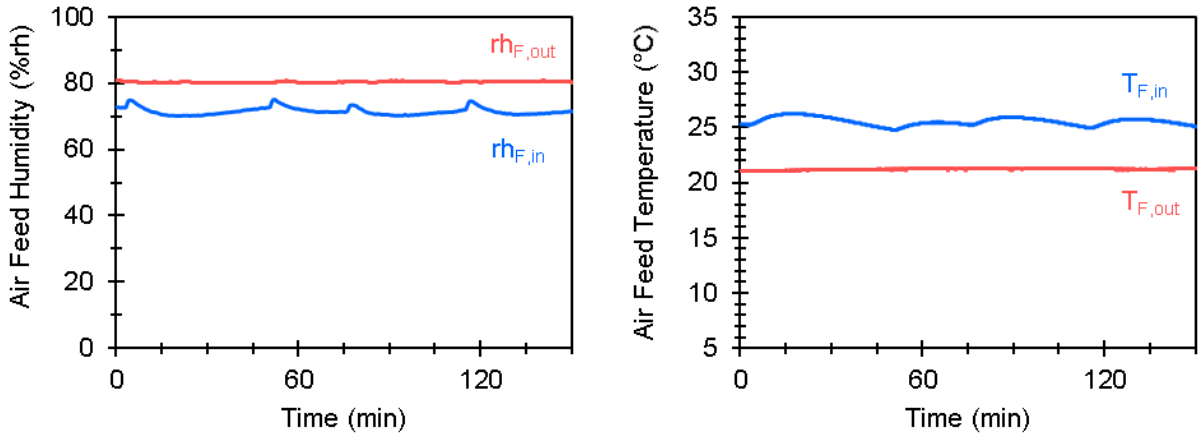

(c) Liquid desiccant temperature at the inlet and outlet as measured by temperature transmitter (800-32/140-11880256, Noshok, Berea, OH).

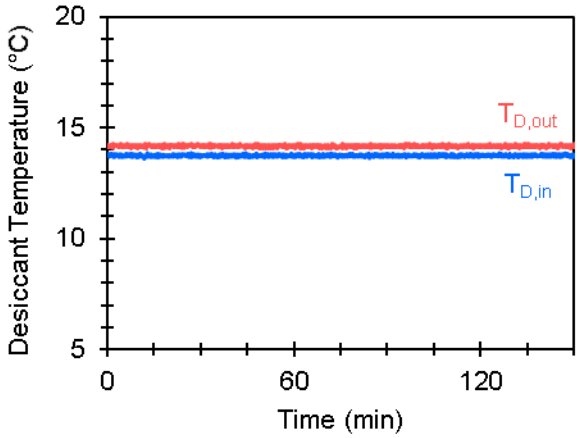

(d) Pressure of the air feed and liquid desiccant as measured by pressure transducer (GC557F0142CD, Ashcroft, Stratford, CT).

S. Moussaddy, S. Aryal, and J. Maisonneuve, "Specific energy analysis of using fertilizer-based liquid desiccants to dehumidify indoor plant environments," Applied Thermal Engineering (in press). https://doi.org/10.1016/j.applthermaleng.2023.121849

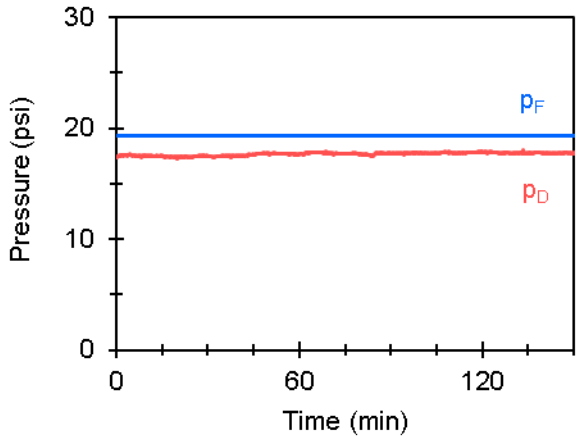

Figure S1. Raw test data.

Table S1. Raw test data and analysis.

Parameter	Value	Measurement or Analysis
Test preparation		
Liquid desiccant water mass $m_{D,w}$	980.4 ± 0.1 g	Balance (AX8201, Ohaus, Parsippany, NJ), 8000 ± 0.1 g
Liquid desiccant salt mass $m_{D,s}$	951.2 ± 0.1 g	Balance (AX8201, Ohaus, Parsippany, NJ), 8000 ± 0.1 g
Liquid desiccant concentration c_D	0.97 ± 0.00014 g/g	$c_D = \frac{m_{D,s}}{m_{D,w}}$ $\frac{\delta c_D}{c_D} = \sqrt{\left(\frac{\delta m_{D,s}}{m_{D,s}}\right)^2 + \left(\frac{\delta m_{D,w}}{m_{D,w}}\right)^2}$
Average trial results		
Air feed flow rate $\dot{V}_F$	4.99 ± 0.05 slpm	Mass flow controller (GH-32907-69, Masterflex, Radnor, PA), 5 slpm ± (0.8 % reading + 0.2 % full scale)
Air feed temperature at inlet $T_{F,in}$	25.5 ± 1 °C	Thermistor temperature sensor (AM2315, Aosong, Guangzhou, China), 125 ± 1 °C

S. Moussaddy, S. Aryal, and J. Maisonneuve, "Specific energy analysis of using fertilizer-based liquid desiccants to dehumidify indoor plant environments," Applied Thermal Engineering (in press). https://doi.org/10.1016/j.applthermaleng.2023.121849

Air feed temperature at outlet $T_{F,out}$	21.1 ± 1 °C	Thermistor temperature sensor (AM2315, Aosong, Guangzhou, China), 125 ± 1 °C
Air feed humidity at inlet $rh_{F,in}$	71.3 ± 2 %rh	Capacitive humidity sensor (AM2315, Aosong, Guangzhou, China), 100 ± 2 %rh
Air feed humidity at outlet $rh_{F,out}$	80.3 ± 2 %rh	Capacitive humidity sensor (AM2315, Aosong, Guangzhou, China), 100 ± 2 %rh
Air feed pressure p_F	17.66 ± 0.38 psi	Pressure transducer (GC557F0142CD, Ashcroft, Stratford, CT), 75 ± 0.38 psi
Liquid desiccant flow rate $\dot{V}_D$	2.08 ± 0.19 slpm	Flowmeter (8051K107, McMaster-Carr, Elmhurst, IL), 1.6 ± 0.05 gpm
Liquid desiccant temperature at inlet $T_{D,in}$	13.7 ± 0.3 °C	Thermal resistance sensor, (800-32/140-1188, Noshok, Berea, OH), 60 ± 0.3 °C
Liquid desiccant temperature at outlet $T_{D,out}$	14.2 ± 0.3 °C	Thermal resistance sensor, (800-32/140-1188, Noshok, Berea, OH), 60 ± 0.3 °C
Liquid desiccant pressure p_D	19.30 ± 0.38 psi	Pressure transducer (GC557F0142CD, Ashcroft, Stratford, CT), 75 ± 0.38 psi
Mass balance analysis		
Water vapor content of air feed at inlet $x_{H2O,in}$	0.015 mol_{H2O}/mol ± 3.56 %	$x_{H2O,in} = rh_{in}\frac{p_{sat,in}}{p_F}$ where $p_{sat,in} = 10^{A-\left(\frac{B}{C+T_{F,in}}\right)}$ $\frac{\delta x_{H2O,in}}{x_{H2O,in}} = \sqrt{\left(\frac{\delta rh_{in}}{rh_{in}}\right)^2 + \left(\frac{\delta p_F}{p_F}\right)^2 + \left(B\ln(10)\frac{\delta T_{F,in}}{(C+T_{F,in})^2}\right)^2}$
Water vapor mass flow of air feed at inlet $\dot{m}_{F,H2O,in}$	3.75 g/h ± 3.76 %	$\dot{m}_{F,H2O,in} = \dot{m}_F\left(\frac{x_{H2O,in}}{1-x_{H2O,in}}\right)\frac{M_{H2O}}{M_{air}}$, $\frac{\delta\dot{m}_{F,H2O,in}}{\dot{m}_{F,H2O,in}} = \sqrt{\left(\frac{\delta\dot{m}_F}{\dot{m}_F}\right)^2 + \left(\frac{\delta x_{H2O,in}}{x_{H2O,in}}\frac{1}{1+x_{H2O,in}}\right)^2}$
Water vapor content of air feed at outlet $x_{H2O,out}$	0.0116 mol_{H2O}/mol ± 3.33 %	$x_{H2O,out} = rh_{out}\frac{p_{sat,out}}{p_F}$ where $p_{sat,out} = 10^{A-\left(\frac{B}{C+T_{F,out}}\right)}$

S. Moussaddy, S. Aryal, and J. Maisonneuve, "Specific energy analysis of using fertilizer-based liquid desiccants to dehumidify indoor plant environments," Applied Thermal Engineering (in press). https://doi.org/10.1016/j.applthermaleng.2023.121849

		$\frac{\delta x_{H2O,out}}{x_{H2O,out}} = \sqrt{\left(\frac{\delta rh_{out}}{rh_{out}}\right)^2 + \left(\frac{\delta p_F}{p_F}\right)^2 + \left(B \ln(10) \frac{\delta T_{F,out}}{(C+T_{F,out})^2}\right)^2}$
Water vapor mass flow of air feed at inlet $\dot{m}_{F,H2O,out}$	2.88 g/h ± 3.53 %	$\dot{m}_{F,H2O,out} = \dot{m}_F \left(\frac{x_{H2O,out}}{1-x_{H2O,out}}\right) \frac{M_{H2O}}{M_{air}}$ $\frac{\delta \dot{m}_{F,H2O,out}}{\dot{m}_{F,H2O,out}} = \sqrt{\left(\frac{\delta \dot{m}_F}{\dot{m}_F}\right)^2 + \left(\frac{\delta x_{H2O,out}}{x_{H2O,out}} \frac{1}{1+x_{H2O,out}}\right)^2}$
Water vapor flux J	0.872 g/m^2/h ± 31.6 %	$J = \frac{\dot{m}_{F,H2O,in} - \dot{m}_{F,H2O,out}}{a}$ where a = 1 m^2 $\delta J = \sqrt{\left(\delta \dot{m}_{F,H2O,in}\right)^2 + \left(\delta \dot{m}_{F,H2O,out}\right)^2}$

S. Moussaddy, S. Aryal, and J. Maisonneuve, "Specific energy analysis of using fertilizer-based liquid desiccants to dehumidify indoor plant environments," Applied Thermal Engineering (in press). https://doi.org/10.1016/j.applthermaleng.2023.121849

Supplementary Note 2: Sample Test Data, Analytical Methods, and Uncertainty Analysis for Validation of the Heat Transport Model

The proposed heat transport model was validated using a series of tests performed on the Oakland University laboratory bench. Figure S2 shows raw data collected for a sample test trial, and Table S2 provides a detailed outline of how data is analyzed, including how experimental uncertainty is propagated throughout the analysis. Heat flux were evaluated by considering a mass and thermal energy balance of the air feed.

(a) Air feed flow rate as measured by mass flow controller (GH-32907-69, Masterflex, Radnor, PA).

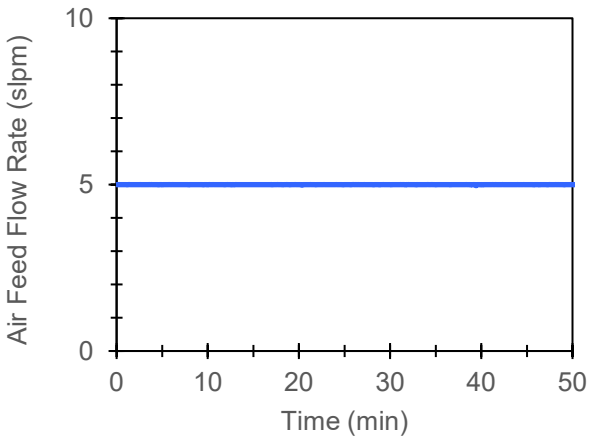

(b) Air feed relative humidity (at specified temperature) at the inlet and outlet as measured by temperature and humidity sensors (AM2315 i2C, Aosong, Guangzhou, China).

S. Moussaddy, S. Aryal, and J. Maisonneuve, "Specific energy analysis of using fertilizer-based liquid desiccants to dehumidify indoor plant environments," Applied Thermal Engineering (in press). https://doi.org/10.1016/j.applthermaleng.2023.121849

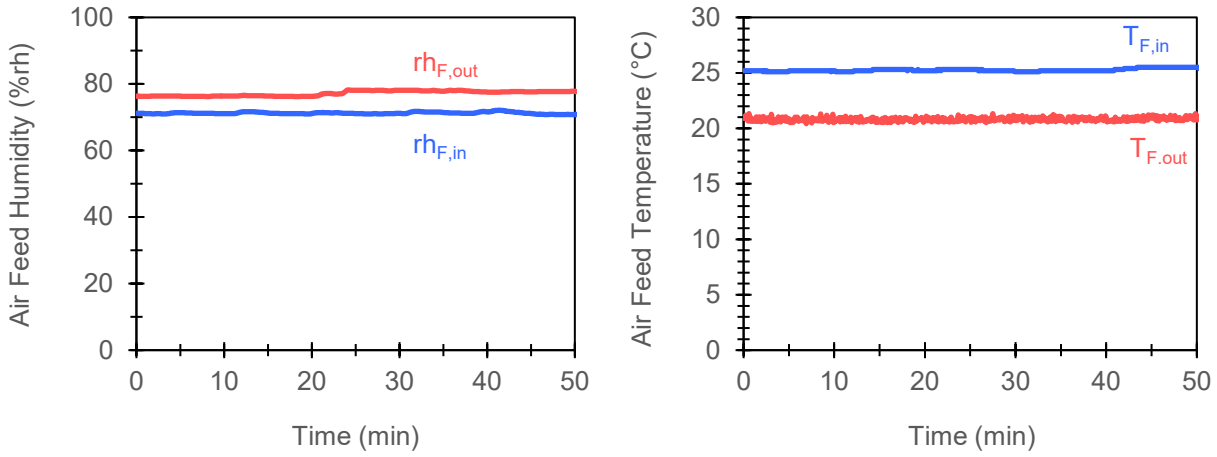

(c) Air feed temperatures at the inlet and outlet of membrane as measured by temperature sensors (MT-6340-30, TWTADE, Suzhou, China)

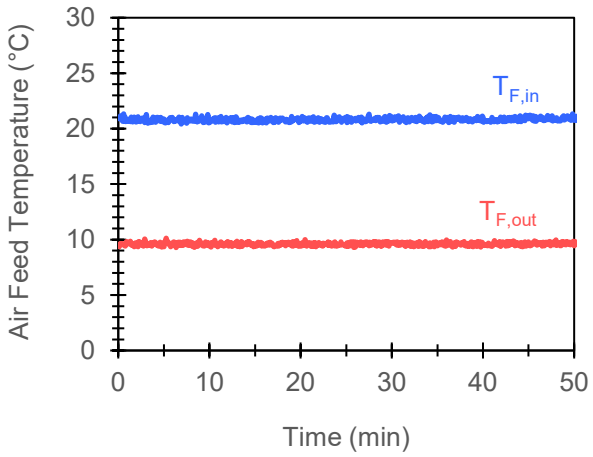

(d) Liquid desiccant temperature at the inlet and outlet as measured by temperature transmitter (800-32/140-11880256, Noshok, Berea, OH).

S. Moussaddy, S. Aryal, and J. Maisonneuve, "Specific energy analysis of using fertilizer-based liquid desiccants to dehumidify indoor plant environments," Applied Thermal Engineering (in press). https://doi.org/10.1016/j.applthermaleng.2023.121849

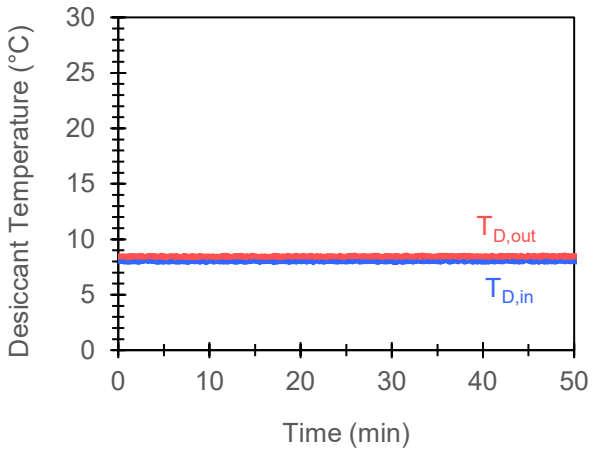

(e) Pressure of the air feed and liquid desiccant as measured by pressure transducer (GC557F0142CD, Ashcroft, Stratford, CT).

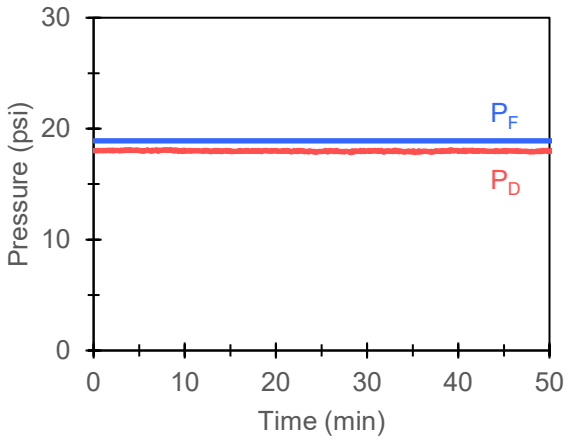

Figure S2. Raw test data.

Table S2. Raw test data and analysis.

Parameter	Value	Measurement or Analysis
Test preparation		
Liquid desiccant water mass $m_{D,w}$	980.4 ± 0.1 g	Balance (AX8201, Ohaus, Parsippany, NJ), 8000 ± 0.1 g

S. Moussaddy, S. Aryal, and J. Maisonneuve, "Specific energy analysis of using fertilizer-based liquid desiccants to dehumidify indoor plant environments," Applied Thermal Engineering (in press). https://doi.org/10.1016/j.applthermaleng.2023.121849

Liquid desiccant salt mass $m_{D,s}$	1.3 ± 0.1 g	Balance (AX8201, Ohaus, Parsippany, NJ), 8000 ± 0.1 g
Liquid desiccant concentration c_D	0.001 ± 0.00014 g/g	$c_D = \frac{m_{D,s}}{m_{D,w}}$ $\frac{\delta c_D}{c_D} = \sqrt{\left(\frac{\delta m_{D,s}}{m_{D,s}}\right)^2 + \left(\frac{\delta m_{D,w}}{m_{D,w}}\right)^2}$
Average trial results		
Air feed flow rate $\dot{V}_F$	4.99 ± 0.05 slpm	Mass flow controller (GH-32907-69, Masterflex, Radnor, PA), 5 slpm ± (0.8 % reading + 0.2 % full scale)
Air feed temperature at inlet $T_{F,in}$	20.82 ± 0.5 °C	Thermal resistance sensor (MT-6340-30, TWTADE, Suzhou, China), 200 °C ± 0.5 °C
Air feed temperature at outlet $T_{F,out}$	9.60 ± 0.5 °C	Thermal resistance sensor (MT-6340-30, TWTADE, Suzhou, China), 200 °C ± 0.5 °C
Air feed humidity at inlet $rh_{F,in}$ @ $T_{rh,in}$	71.2 ± 2 %rh @ 25.25 ± 0.1 °C	Capacitive humidity sensor (AM2315, Aosong, Guangzhou, China), 100 ± 2 %rh
Air feed humidity at outlet $rh_{F,out}$@ $T_{rh,out}$	77.2 ± 2 %rh @ 19.81 ± 0.1 °C	Capacitive humidity sensor (AM2315, Aosong, Guangzhou, China), 100 ± 2 %rh
Air feed pressure p_F	17.9 ± 0.38 psi	Pressure transducer (GC557F0142CD, Ashcroft, Stratford, CT), 75 ± 0.38 psi
Liquid desiccant flow rate $\dot{V}_D$	2.08 ± 0.19 slpm	Flowmeter (8051K107, McMaster-Carr, Elmhurst, IL), 1.6 ± 0.05 gpm
Liquid desiccant temperature at inlet $T_{D,in}$	8.02 ± 0.3 °C	Thermal resistance sensor, (800-32/140-1188, Noshok, Berea, OH), 60 ± 0.3 °C
Liquid desiccant temperature at outlet $T_{D,out}$	8.45 ± 0.3 °C	Thermal resistance sensor, (800-32/140-1188, Noshok, Berea, OH), 60 ± 0.3 °C
Liquid desiccant pressure p_D	18.9 ± 0.38 psi	Pressure transducer (GC557F0142CD, Ashcroft, Stratford, CT), 75 ± 0.38 psi

S. Moussaddy, S. Aryal, and J. Maisonneuve, "Specific energy analysis of using fertilizer-based liquid desiccants to dehumidify indoor plant environments," Applied Thermal Engineering (in press). https://doi.org/10.1016/j.applthermaleng.2023.121849

Mass balance analysis		
Water vapor content of air feed at inlet $x_{H2O,in}$	0.0177 mol_{H2O}/mol ± 3.52 %	$x_{H2O,in} = rh_{in}\,\frac{p_{sat,in}}{p_F}$ where $p_{sat,in} = 10^{A-\left(\frac{B}{C+T_{F,in}}\right)}$ $\frac{\delta x_{H2O,in}}{x_{H2O,in}} = \sqrt{\left(\frac{\delta rh_{in}}{rh_{in}}\right)^2 + \left(\frac{\delta p_F}{p_F}\right)^2 + \left(B\ln(10)\frac{\delta T_{F,in}}{(C+T_{F,in})^2}\right)^2}$
Water vapor mass flow of air feed at inlet $\dot{m}_{F,H2O,in}$	4.22 g/h ± 3.74 %	$\dot{m}_{F,H2O,in} = \dot{m}_F\left(\frac{x_{H2O,in}}{1-x_{H2O,in}}\right)\frac{M_{H2O}}{M_{air}}$, $\frac{\delta \dot{m}_{F,H2O,in}}{\dot{m}_{F,H2O,in}} = \sqrt{\left(\frac{\delta \dot{m}_F}{\dot{m}_F}\right)^2 + \left(\frac{\delta x_{H2O,in}}{x_{H2O,in}}\frac{1}{1+x_{H2O,in}}\right)^2}$
Water vapor content of air feed at outlet $x_{H2O,out}$	0.013 mol_{H2O}/mol ± 2.84 %	$x_{H2O,out} = rh_{out}\frac{p_{sat,out}}{p_F}$ where $p_{sat,out} = 10^{A-\left(\frac{B}{C+T_{F,out}}\right)}$ $\frac{\delta x_{H2O,out}}{x_{H2O,out}} = \sqrt{\left(\frac{\delta rh_{out}}{rh_{out}}\right)^2 + \left(\frac{\delta p_F}{p_F}\right)^2 + \left(B\ln(10)\frac{\delta T_{F,out}}{(C+T_{F,out})^2}\right)^2}$
Water vapor mass flow of air feed at outlet $\dot{m}_{F,H2O,out}$	3.27 g/h ± 3.05 %	$\dot{m}_{F,H2O,out} = \dot{m}_F\left(\frac{x_{H2O,out}}{1-x_{H2O,out}}\right)\frac{M_{H2O}}{M_{air}}$ $\frac{\delta \dot{m}_{F,H2O,out}}{\dot{m}_{F,H2O,out}} = \sqrt{\left(\frac{\delta \dot{m}_F}{\dot{m}_F}\right)^2 + \left(\frac{\delta x_{H2O,out}}{x_{H2O,out}}\frac{1}{1+x_{H2O,out}}\right)^2}$
Water vapor flux J	0.95 $g/m^2/h$ ± 19.7 %	$J = \frac{\dot{m}_{F,H2O,in}-\dot{m}_{F,H2O,out}}{a}$ where a = 1 m^2 $\delta J = \sqrt{\left(\delta \dot{m}_{F,H2O,in}\right)^2 + \left(\delta \dot{m}_{F,H2O,out}\right)^2}$
Energy balance analysis		
Heat flux $\dot{q}$	1.84 W/m^2 ± 8.7 %	$\dot{q} \approx \frac{\dot{m}_F\, c_p\left(T_{F,in} - T_{F,out}\right) + \left(\dot{m}_{F,H2O,in} - \dot{m}_{F,H2O,out}\right) H_c}{a}$ Where H_c = 2501 J/g

S. Moussaddy, S. Aryal, and J. Maisonneuve, "Specific energy analysis of using fertilizer-based liquid desiccants to dehumidify indoor plant environments," Applied Thermal Engineering (in press). https://doi.org/10.1016/j.applthermaleng.2023.121849

$$\delta\dot{q} = \left(\left(\delta\dot{m}_F \frac{c_p\left(T_{F,in} - T_{F,out}\right)}{a}\right)^2 + \left(\delta T_{F,in} \frac{\dot{m}_F\, c_p}{a}\right)^2 + \left(-\delta T_{F,out} \frac{\dot{m}_F\, c_p}{a}\right)^2 + \left(\delta\dot{m}_{F,H2O,in} \frac{H_c}{a}\right)^2 + \left(\delta\dot{m}_{F,H2O,out} \frac{H_c}{a}\right)^2\right)^{1/2}$$